PHYSICAL REVIEW B VOLUME 20, NUMBER 1 1 JULY 1979

Monte Carlo study of the spatially modulated phase in an Ising model

Walter Selke* and Michael E. Fisher
Baker Laboratory, Cornell University, Ithaca, New York 14853
(Received 16 February 1979)

The spatially modulated or "sinusoidal" phase which occurs in a three-dimensional spin-$\frac{1}{2}$ Ising model with competing ferromagnetic and antiferromagnetic interactions between adjacent and next-nearest xy layers is studied by Monte Carlo methods. The equilibrium wave vector, $q(T)$, changes, possibly with jumps, from $q=\pi/2a$ at $T=0$, to its near-critical value: for $-J_2/J_1=0.6$, the change occurs rapidly in the interval 0.8 T_c to 0.9 T_c. The magnetization wave form appears to display distinct, although small, third harmonic components up to T_c.

I. INTRODUCTION

In this article we study the low temperature, spatially modulated phase of a three-dimensional simple cubic-lattice Ising model with competing interactions between nearest layers and next-nearest layers (perpendicular to the z axis). The model was introduced some years ago[1,2] to describe the magnetic properties of erbium, which displays a sinusoidally ordered low-temperature phase.[3] The original theoretical analysis was restricted to mean-field-type calculations leading, among other conclusions, to a sinusoidally ordered phase with an essentially temperature-independent wave vector determined only by the ratio of the two competing exchange integrals. Higher harmonics were predicted to appear below approximately one half of the transition temperature. These theoretical results have been used to interpret experimental data on erbium, thulium, and some of their alloys[4] with apparent but, as will become evident below, really misleading success.

Recently there has been a renewed interest in the model because it displays a Lifshitz point,[5] namely, a multicritical point separating a uniformly ordered phase, a modulated or "sinusoidally" ordered phase, and a disordered phase. The new theoretical treatments,[6,7] however, have been limited mainly to the properties close to the phase transition temperatures, modifying the mean-field results only quantitatively, specifically: shifting the location of the Lifshitz point, and giving more precise values for the critical lines, the critical exponents, and the critical wave vector as a function of the competing interactions. No serious attempts seem to have been made to analyze the sinusoidal phase itself in any detail[8] although consideration of the discrete, Ising nature of the spins stimulates a number of questions about the possible nature of a modulated phase in the model, particularly as the temperature is lowered towards zero where, clearly, an incommensurate, near-sinusoidal state cannot easily be realized. Thus the variation with temperature of the equilibrium wave vector $q(T)$, and of the harmonic content of the magnetization modulation are of paramount interest.

The layout of this article is as follows: The model is defined explicitly and the phase diagram and the ground state are discussed in Sec. II. Then the results of some Monte Carlo calculations are presented. The ambiguities, advantages, and drawbacks of various boundary conditions in the Monte Carlo study are sketched briefly; furthermore, various dynamic mechanisms occurring in the sinusoidal phase, within the stochastic kinetics of the Monte Carlo process, are displayed in Sec. III. In Sec. IV, the dramatic dependence of the wave vector on the temperature (for a fixed value of the ratio of the exchange integrals) is demonstrated. In Sec. V the magnetization waves are Fourier-analyzed and the role of the higher harmonics is discussed. Finally, the results are summarized briefly.

II. THE MODEL AND ITS PHASE DIAGRAM

We consider a spin-$\frac{1}{2}$ Ising model on a simple cubic lattice of $L\times M\times N$ sites with ferromagnetic interactions ($J_0>0$) between each spin at site (x,y,z) ($s_{x,y,z}=\pm 1$) and its nearest neighbors in the xy planes, and competing interactions between the spins in adjacent layers J_1, and in the next-nearest layers J_2; see Fig. 1(a). Explicitly, the Hamiltonian may be written

$$\mathcal{H}=-\frac{1}{2}\sum_{x,y,z}\left(J_0 s_{x,y,z}s_{x\pm 1,y\pm 1,z}+J_1 s_{x,y,z}s_{x,y,z\pm 1}+J_2 s_{x,y,z}s_{x,y,z\pm 2}\right), \quad (1)$$

where x, y, and z run over integer values, i.e., we take a lattice spacing $a\equiv 1$.

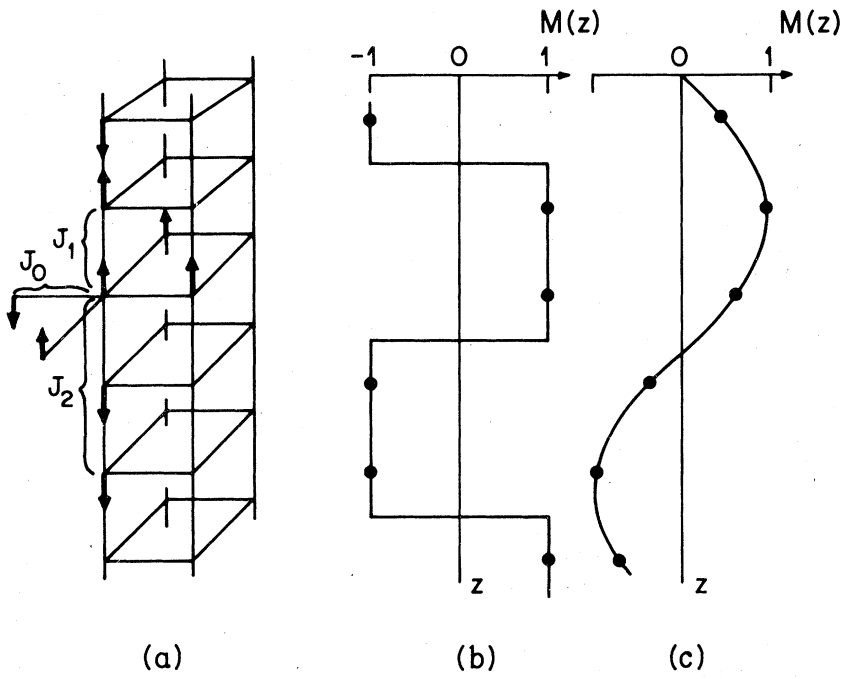

FIG. 1. (a) Ising model with ferromagnetic interactions of strength J_0 in the layers and competing interactions between nearest, J_1, and next-nearest layers, J_2. (b) Magnetization per layer, $M(z)$ for the (2,2) antiphase state ($T=0$, $|J_2| > \frac{1}{2}|J_1|$). (c) Magnetization per layer in a sinusoidal structure of large amplitude.

For reasons of brevity and simplicity we will assume $|J_1| = J_0$. We will always presuppose the thermodynamic limit ($L,M,N \to \infty$) unless otherwise stated. We will disregard the cases (i) $J_1, J_2 > 0$ and (ii) $J_1 < 0$ and $J_2 > 0$, since these yield only ferromagnetically or antiferromagnetically (metamagnetically) ordered phases, whatever the relative values of J_1 and J_2. Indeed, a sinusoidally ordered phase can be achieved only if (iii) both exchange integrals are of antiferromagnetic sign, $J_1, J_2 < 0$, or if (iv) J_1 is positive (ferromagnetic) while J_2 represents a competing antiferromagnetic interaction. In the Appendix we prove, by means of the transfer matrix method, that at zero temperature in case (iii) the antiferromagnetic state is the stable one only for $|J_2/J_1| < 0.5$, while in case (iv) the ferromagnetic state is stable only for $|J_2|/J_1 < 0.5$. In both cases for all other values of the ratios, the ground state of an infinite system is periodic, with a period of four lattice spacings, and is represented by a sequence of two layers of up-spins ($s_{x,y,z} = +1$) followed by two layers of down-spins ($s_{x,y,z} = -1$), etc., i.e., by a configuration sometimes called a (2,2) antiphase state [see Fig. 1(b)].

A fair description near the critical line may be obtained by a mean-field calculation.[6] In both cases, (iii) and (iv), one finds for $T \lesssim T_c$, a "sinusoidal" spin configuration [Fig. 1(c)] in the ordered phase for $|J_2/J_1| > 0.25$, and a ferromagnetic, or antiferromagnetic, configuration, respectively, for smaller values of $|J_2/J_1|$. The mean-field transition temperature is given by[1]

$$k_B T_c^{\mathrm{MF}} = 4|J_1| + 2J_1 \cos q_0^{\mathrm{MF}} + 2J_2 \cos 2q_0^{\mathrm{MF}} \quad , \tag{2}$$

where q_0^{MF} is the wave vector describing the magnetization per spin in a layer as

$$M(z) \equiv \frac{1}{LM} \sum_{x,y} \langle s_{x,y,z} \rangle = M_0(T) \cos(q_0^{\mathrm{MF}} z + \phi) \quad , \tag{3}$$

near T_c and is given explicitly by

$$q_0^{\mathrm{MF}} = \cos^{-1}(-J_1/4J_2) \quad , \tag{4}$$

for $|J_2/J_1| > 0.25$, and $q_0^{\mathrm{MF}} \equiv 0$ (ferromagnetic case) or $q_0 = \pi$ (antiferromagnetic case) for smaller ratios. In Eq. (3) the phase ϕ, is arbitrary.

In case (iv) these results have been essentially confirmed by the high-temperature series expansion[6] and previous Monte Carlo calculations[7] with only a comparatively small shift in the value separating the sinusoidal and the ferromagnetic phase, to $|J_2/J_1| \simeq 0.27$, and reductions in $T_c(J_2/J_1)$ of about 30–40%. (For a more detailed comparison, see Ref. 6.) The results for $T_c(J_2/J_1)$ and for the ground state are summarized in the phase diagram in Fig. 2.

In the following, we restrict our analysis mainly to

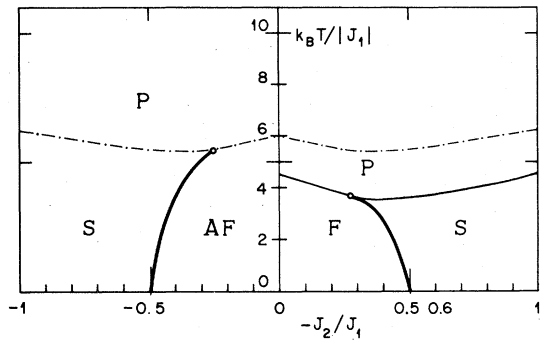

FIG. 2. Phase diagram showing the transition lines between the sinusoidal (S), ferromagnetic (F), antiferromagnetic (AF), and paramagnetic (P) phases. The dot-dash lines represent the results of mean-field theory; the thin solid line is taken from the high-temperature series expansion; the location of the first-order transitions, denoted by thick lines, is schematic and, indeed, the precise nature of the S/F and S/AF phase boundaries has not yet been established convincingly.

the fixed ratio $J_2/J_1 = -0.6$, so that the sinusoidal phase should be realized for all temperatures below T_c. Our analysis utilizes the Monte Carlo method for a finite system of size $L \times M \times N$; N corresponds to the z direction, so specifying the number of layers.

III. THE MONTE CARLO METHOD

A. Boundary conditions

In this section, we discuss the role of the boundary conditions for the Monte Carlo calculations. Usually, one has to choose between periodic boundary conditions (pbc) or "free surface" conditions (i.e., putting interactions across the surface of the finite system equal to zero), antiperiodic boundary conditions, or the "self-consistent effective field"-boundary condition.[9] In our study, we have not used the last two possibilities. Antiperiodic boundary conditions have been shown to be useful mainly for problems involving an interface, although they are not actually inconsistent with a (2,2) antiphase ground state. The self-consistent field boundary conditions have so far been defined only for systems with a simple order parameter.[10] Although they might be valuable in the present problem, we have not seen how to define them with sufficient generality.

Since the expected sinusoidal magnetization pattern has a modulation only in the z direction, the boundary conditions for the ferromagnetically coupled xy layers are not crucial. Accordingly, in order to simulate an infinite system most closely, periodic boundary conditions across the layers are appropriate and have been adopted.

To allow for a freely variable wavelength of the magnetization pattern in the z direction, one is led to considering seriously free boundary conditions at the planes $z = 1$ and $z = N$. However, we find that taking free surfaces in the z direction leads to a pinning effect, i.e., a tendency to have a broad maximum or minimum in the magnetization $M(z)$, at the surface. We have observed this pinning effect in all our runs, using systems of the sizes $6 \times 6 \times 40$ and $10 \times 10 \times 40$. In fact, the pinning effect can be explained for the Hamiltonian (1) quite easily. First, for the two surface layers the ferromagnetic interactions in the layers are enhanced relative to the interactions in the z direction, since antiferromagnetic couplings are missing. Second, the energy for the surface layers, having unsaturated interactions, is smaller for a sequence of (at least two) layers with spins having the same sign than for one with spins with alternating signs. This explains the broadness of the minima or maxima. For a system of sufficient length, N, in the z direction, relative to the wavelength of the magnetization pattern, the pinning effect should not spoil the "bulk" behavior significantly. However, we encounter wavelengths of from four to seven lattice spacings, for which the computationally feasible values of N are not very large. Accordingly, we have preferred to use for most of our calculations simple periodic boundary conditions also in the z direction.

Certainly the use of periodic boundary conditions avoids any pinning effects. On the other hand, the wavelength of any equilibrium pattern found will necessarily be commensurate with the length N (even though the wavelength may, and, in fact, does change during approach to statistical equilibrium). On the other hand, there is some computational advantage in having only a well-defined series of possible wave vectors. The series can be refined by choosing different lengths of the system, as will be seen in Sec. IV. Despite this, there does seem to be a need for some new type of boundary conditions for dealing with periodic structures. (Although we have some ideas to offer in this connection, we have not investigated or tested them.)

B. Kinetic processes

During the course of the Monte Carlo calculations one approaches and simulates the equilibrium by a kinetic process described by a master equation.[9] Thereby the method can give information about dynamic phenomena occurring in the system studied, although one has to be aware that the stochastic kinetics may be quite unrealistic for many physical systems. By taking the ground state, i.e., the (2,2) antiphase state, as the initial configuration of a Monte Carlo run one may simulate a heating process. On the other hand, starting with the ferromagnetic, or fully aligned ground state, we may observe effects

associated with the turning off of a strong magnetic field.

The most interesting effect we have observed by heating the system is a "squeezing" phenomenon. In this, two neighboring maxima or minima move together and merge so that the overall wavelength is changed. A sequence of graphs picturing this effect (for parameters: $6\times6\times40$; pbc; $k_BT=3.025J_1$, $-J_2/J_1=0.6$) are displayed in Fig. 3. The intermediate steps of the squeezing can best be detected by taking a small number ($\lesssim30$) of Monte Carlo steps per spin (MCS/S) in calculating the average $M(z)$: in Fig. 3 averages were computed over 20 MCS/S. Actually, the squeezing effect occurred three times in the full approach to equilibrium in the run sampled in Fig. 3, thereby changing the wavelength from 4 to $40/7\simeq5.71$, at equilibrium. By looking at instantaneous configurations in equilibrium one finds fairly harmonic sine waves, the distortions becoming even smaller for a larger number of spins, say 10×10 xy layers instead of 6×6 layers. This suggests that the sine waves are effectively present at all times and are not just a result of a very long time averaging procedure. Considering the discrete Ising character of the spins, this is quite surprising.

The squeezing effect also occurs when using free surface conditions. However, in that case a "free expansion" mechanism can also be observed, i.e., an increase of the wavelength due to the wave's "moving out of the surface". The free expansion can be understood by calculating the energies necessary to overturn various layers of spins. In Fig. 4 we show the sequence of spin flips associated with the energetically most favorable steps near a surface. In fact, the free expansion effect was found to be the dominant mechanism in the later stages of the Monte Carlo runs as equilibrium was approached.

The kinetics involved in turning off a strong magnetic field seem to be quite different. Indeed, for the heating process it takes about 300–350 MCS/S to destroy three waves and establish equilibrium (for parameters $6\times6\times40$; $k_BT/J_1=3.025$; pbc). However, on starting from the fully magnetized state with the same parameters, sine waves of close-to-equilibrium wavelength evolve almost simultaneously in the first 30–50 MCS/S; final equilibrium, however, still required a further 200 to 300 MCS/S.

In equilibrium we observe a drift of the sine waves in the case of pbc. This drift may be described quantitatively by the change of the phase at the surface per MCS/S. For $-J_2/J_1=0.6$ we find an increase of the drift in going from $k_BT/J_1=3.025$ ($6\times6\times40$) to $k_BT/J_1=3.402$, by a factor of about 4, i.e., the sine waves fluctuate more rapidly closer to T_c. This drift or fluctuation has to be taken into account in defining a reasonable averaging procedure to determine the amplitude of the magnetization modulation.

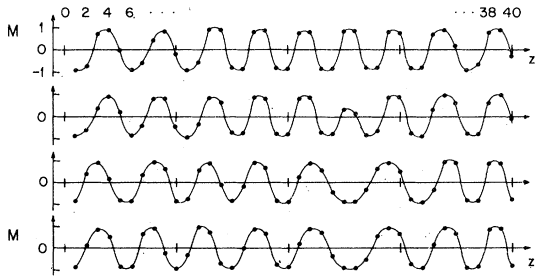

FIG. 3. Sequence of magnetization plots showing the squeezing effect in a $6\times6\times40$ system at $k_BT=3.025\ J_1$. The evolution of the magnetization per layer, $M(z)$, in a single run between 180 and 260 MCS/S (averages are taken over 20 MCS/S) is shown. [Note that MCS/S means Monte Carlo steps per spin.]

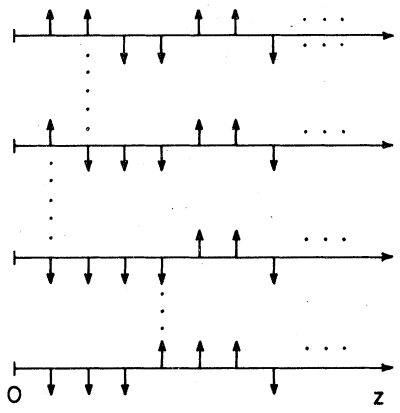

FIG. 4. Sequence of spin configurations near the surface (at $z=0$) associated with the energetically most favorable spin flips, showing an expansion of the wavelength.

IV. TEMPERATURE DEPENDENCE OF THE WAVE VECTOR

Because of the significantly different values of the equilibrium wave vector $q(T)$, in the ground state and near T_c (see Fig. 5) there must be quite a large temperature dependence of the wave vector, contrary to the findings of the earlier mean-field theory treatments. In the special case, $-J_2/J_1=0.6$, one expects a change from a wave vector $q=\frac{1}{2}\pi\simeq1.57$ at $T=0$, to a wave vector $q=q_c\simeq1.13$ at T_c, where for the infinite system, $k_BT_c/J_1=3.82\pm0.02$, according to the high-temperature series extrapolations. In order to approximate these two values reasonably closely, we have used $N=40$ and $N=56$. Because we are using pbc we are then taking into account the two series of wave vectors $q=2\pi k/40$ and $q=2\pi k/56$,

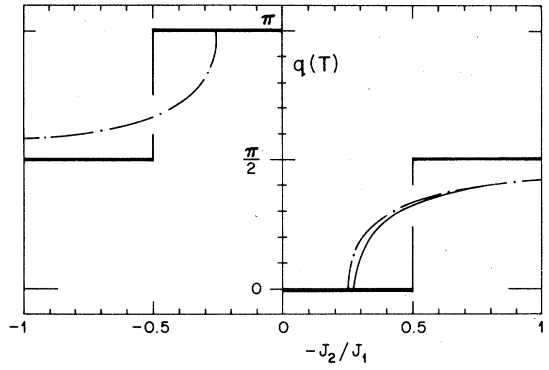

FIG. 5. Plot of the equilibrium wave vector q vs the ratio of the exchange integrals, $-J_2/J_1$. The bold lines refer to the ground state. The dot-dash curve gives the critical wave vector according to mean-field theory; the solid curve reproduces the high-temperature series extrapolation results of Ref. 6.

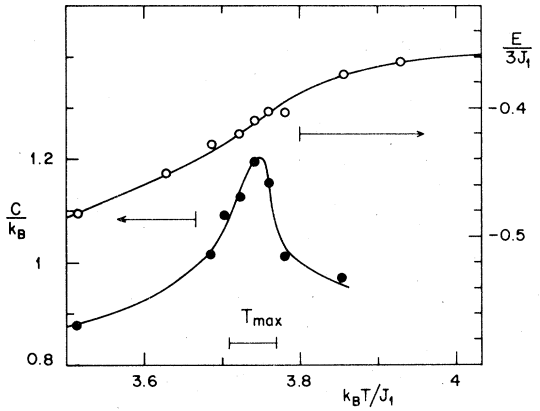

FIG. 6. Plot for a $10\times10\times40$ system of the specific heat per spin C (calculated from the total energy fluctuation) and of the energy per spin, E, vs temperature. Note that $J_1\equiv J_0$ is used to scale the variables. The solid curves serve merely as a guide to the eye: the estimate for T_{max} is indicated.

respectively, with k being an integer representing the number of complete waves. The expected limiting values for q are obtained for $k=10,7$ and $k=14,10$, respectively.

In the light of the well-known finite size effects[11] we have also varied the number $(L\times M;L=M)$ of spins of the xy layers. For the $6\times6\times40$ and the $10\times10\times40$ Monte Carlo systems we have estimated the "ordering temperature" T_{max}, by the location of the maxima of the specific heat and the turning points of the energy per spin: See Fig. 6, which shows data for the $10\times10\times40$ system. For the smaller block one obtains $k_BT_{max}/J_1=3.63\pm0.03$, for the larger one $k_BT_{max}/J_1=3.74\pm0.03$. A qualitatively similar increase of T_{max} for larger finite systems has been observed for the usual three-dimensional Ising model.[12] To get a quantitative picture, one should use the appropriate finite size scaling theory. To our knowledge, however, quantitative results are available only for systems, where one varies either all linear dimensions $(L=M=N)$ simultaneously[12,13] or only one linear dimension, say N, taking the other two to be infinite.[14] In the first case, the ordering temperature approaches its limiting value as $N^{-\lambda}$, where the shift exponent λ is given as the inverse of the canonical critical exponent ν.[11] In the latter case one finds[14(b)] $\lambda\simeq2$ for pbc. In our instance, two linear dimensions are changed at the same time $(L=M)$, the third dimension N, being fixed and moderately large, but certainly not infinite. The corresponding finite size scaling behavior is not known exactly; thus for the purposes of rough estimation we have incorporated in Fig. 7 the two extreme shift exponents $\lambda=2$ and $\lambda=1.4$ (the last corresponding to the largest expected value of ν; note the argument[15] that the transition from the sinusoidal to the paramagnetic phase should be described by the critical exponents of the XY model or $n=2$ symmetry). At any rate, we obtain a rough estimate (see Fig. 7) $k_BT_c/J_1=3.82\pm0.03$, for the transition temperature of the infinite system, which is in embarrassingly close agreement with the high-temperature series expansion estimate of 3.82 ± 0.02 for the same ratio $-J_2/J_1=0.6$.

In Fig. 8 we show some equilibrium configurations, averaged over about 90 MCS/S, for the magnetization per layer $M(z)$ as a function of temperature for the $6\times6\times40$ system. One sees that the wave vector may be determined merely by counting the number of wave crests or maxima. The results, for all sys-

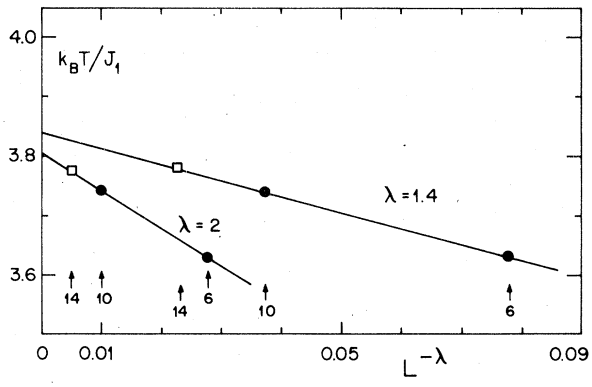

FIG. 7. Variation of the "ordering temperature", T_{max}, for $L\times L\times40$ systems. The trial exponents $\lambda=1.4$ and $\lambda=2$ are discussed in the text.

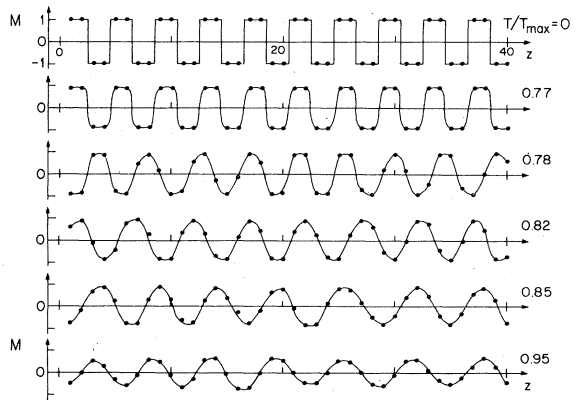

FIG. 8. Equilibrium configurations for the magnetization per layer $M(z)$ (averaged over about 90 MCS/S) for the $6\times6\times40$ system. The reduced temperature T/T_{max}, with $k_B T_{max}=3.63\ J_1$, is marked on the right.

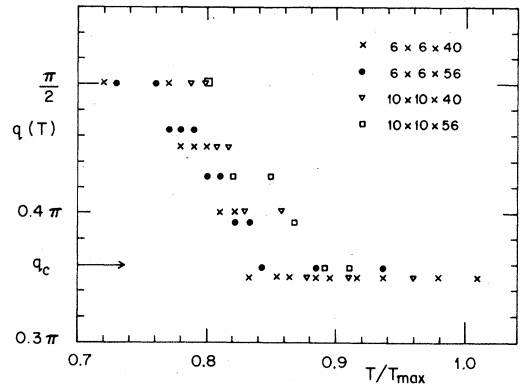

FIG. 9. Wave vector $q(T)$ vs the reduced temperature, T/T_{max}, for the system sizes indicated. (The dependence of T_{max} on $N=40$ or 56 has been neglected.) The arrow indicates the critical value, q_c, according to the high-temperature series analysis (Ref. 6).

tems considered ($6\times6\times40$, $10\times10\times40$, $6\times6\times56$, and $10\times10\times56$) are summarized in Fig. 9, where the wave vector $q(T)$ is plotted versus T/T_{max}, where T_{max} refers to the ordering temperatures of the systems with $N=40$, i.e., we assume only a weak dependence of T_{max} on N in accordance with our findings within the finite size scaling analysis. The results shown have been obtained by runs of at least 700 MCS/S; for some temperatures near the apparent jumps in $q(T)$, as many as 2000 MCS/S were used.

We may summarize Fig. 9 in the following way: obviously, there is a rather dramatic change of the wave vector in a comparatively small temperature range between about 80 and 90% of the transition temperature. Certainly, we cannot decide from the present study whether, for an infinite system, this change occurs in a sequence of commensurable wave vectors (as here forced by the pbc) or by a continuous change of the wave vector, as would be true for the analogous wave vector determined by the maximum in the structure factor for the corresponding one-dimensional Ising model. An interesting question is, whether there are certain plateaus, regions in which the wave vector changes only by a small amount over a relatively large temperature region or, perhaps, even locks in, at a constant value, a behavior apparently observed for erbium,[3] e.g. Our results, especially for the $10\times10\times40$ and $10\times10\times56$ systems, certainly do not contradict such a staircase-like behavior near $q=\frac{2}{5}\pi$.[8] We remark also that there are theoretical grounds for believing that the ground state value $q(0)=\frac{1}{2}\pi$ probably does lock in below some definite temperature.

In concluding this section, a word of caution may be appropriate. Starting from an equilibrium configuration with $q=\frac{7}{20}\pi$, we were not able to reach in a reasonable computing time (4000 MCS/S in a $6\times6\times40$ system) the state at a lower temperature with the appropriate new and distinct wave vector expected from the data obtained by "heating" the ground state as described above. Instead, the old, high-temperature wave vector appeared to lock in. This behavior could, however, correspond to a genuine metastability of the sort which has been seen experimentally in the form of hysteresis effects.

V. FOURIER ANALYSIS AND HIGHER HARMONICS

Using $N=40$ as the length of periodicity, one can express the magnetization per layer $M(z)$ in a Fourier series as

$$M(z)=\sum_{k=1}^{N}\left[a_k\cos(2\pi kz/N)+b_k\sin(2\pi kz/N)\right]\ . \tag{5}$$

Recall that $M(z)$ is defined only for the discrete values of $z=1,\cdots N$. The coefficients a_k and b_k are simply

$$a_k=\frac{2}{N}\sum_{z=1}^{N}M(z)\cos\left(\frac{2\pi kz}{N}\right)\ , \tag{6}$$

$$b_k=\frac{2}{N}\sum_{z=1}^{N}M(z)\sin\left(\frac{2\pi kz}{N}\right)\ . \tag{7}$$

We have calculated these coefficients by taking the average for $M(z)$ in equilibrium over 20 MCS/S and then repeating this averaging at least 36 times. This

procedure takes into account the small time scale fluctuations of the waves mentioned previously. The long time drifts can be eliminated by studying $(a_k^2+b_k^2)^{1/2}$ instead of a_k and b_k separately.

In order to determine the harmonic content of the magnetization wave forms, we have plotted $(a_k^2+b_k^2)^{1/2}$ vs k as illustrated in Fig. 10. Certainly, as regards the dominant wave vector, the results are completely consistent with those presented in Sec. IV. In other words, Fourier analysis confirms what is found simply by counting the number of visible wave crests or maxima. More interestingly, there seems to be a systematic dependence of the line shape of the leading (or "first") harmonic on the size of the system. For $T/T_{\max}=0.93$ we have examined the sizes $L=M=6$, 10, and 14. The line shapes were analyzed in two ways: first a power-law behavior of the line shape was tested by plotting on a double-logarithmic scale $(a_k^2+b_k^2)^{1/2}$ vs $(2\pi k/q)-1$, where $q=q(T)$ denotes the location of the leading harmonics as before. Only a weak dependence of the exponent, say θ, on L appears: indeed, all three cases can be reasonably described by $\theta=3.1\pm0.3$. This power-law behavior is reminiscent of that observed experimentally for the structure factor in the smectic-A phases of a liquid crystal.[16] There, it arises from the fluctuations of a one-dimensional density wave which corresponds in the spin model to the one-dimensional modulation of magnetization, along the z direction. On the other hand, we are *not* really calculating the structure factor, but only the Fourier transform of the average magnetization per layer. Indeed, if one plots $(a_k^2+b_k^2)^{1/2}$ vs $1/L$ for fixed values of k, the same effective temperature $T/T_{\max}$, and the three values $L=6$, 10, and 14, a linear extrapolation suggests the vanishing of $(a_k^2+b_k^2)^{1/2}$ for all values of k corresponding to a wave vector not equal to $q(T)$ in the limit $L\to\infty$. While it would be desirable to calculate the structure factor for the magnetic model, this is computationally very expensive.

Evidently (see Fig. 10), Fourier analysis reveals the existence of a nonvanishing third harmonic: indeed, for the $14\times14\times40$ system the third harmonic persists even up to $0.93T_{\max}$ (i.e., $k_BT/J_1=3.515$, the highest temperature studied). The location of the third harmonics in the figures may be surprising at first sight; however, it reflects simply the periodicity length, N, of the system.[17] In the case of $q=2\pi(\frac{8}{40})$, which arises, e.g., for $T/T_{\max}=0.829$ (not shown in Fig. 10), one cannot distinguish between the second and third harmonics. However, in the light of the other results, and the theoretical analysis by Miwa and Yosida,[18] one can, nonetheless, safely identify the observed peak at $k=16$ as indicative of the third harmonic.

Quantitatively, the mean-field analyses[18,19] predict a decrease of the amplitude of the third harmonic according to $(T_c-T)^{3/2}$. We did not try to test this prediction, because the finite size "background" is too large. Furthermore, we could not detect higher odd harmonics within the precision of the Monte Carlo study for $T>0.8\ T_c$, although these are also expected theoretically and are evident from the $M(z)$ plots below $0.75\ T_c$. What is rather surprising, however, and also evident from Fig. 8, is that even when the maxima in the magnetization wave forms are close to saturation ($M_{\max}=0.90$ to 0.95) the amplitude of the higher harmonics for the states with $q<q(0)=\frac{1}{2}\pi$ is quite small, and the wave forms are rather close to pure sinusoids. Indeed, this conclusion remains true even if the instantaneous configurations for the $6\times6\times N$ lattices are examined. Furthermore, the clusters of overturned spins in adjacent layers appear to exhibit rather little correlation. For $q<q(0)$, therefore, a picture in which each layer orders more or less independently in the mean field provided by its adjacent and next-nearest layers[8] may have a greater range of validity than might be anticipated on *a priori* grounds.

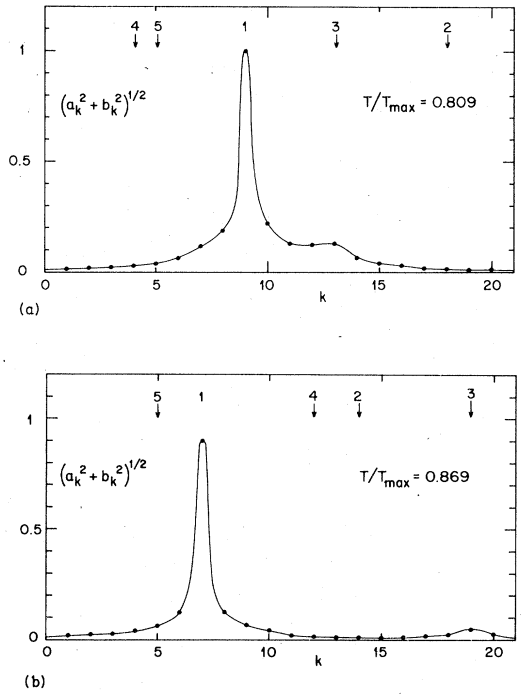

FIG. 10. Fourier coefficients, $(a_k^2+b_k^2)^{1/2}$, of the magnetization vs wave index k for a $10\times10\times40$ system at two temperatures (with $k_BT_{\max}=3.74\ J_1$). The labelled arrows indicate the positions at which various harmonics may appear. A plot for $T/T_{\max}=0.829$ resembles (b) except for the location of the peaks, which are now at $k=8$ and $k=16$.

VI. SUMMARY

We have studied the modulated phase in a three-dimensional Ising model with competing interactions between layers ($J_1 > 0$, $J_2 < 0$) using, in particular, a Monte Carlo approach. Different boundary conditions on finite systems have been compared, leading to the selection of periodic boundary conditions to get a well-defined sequence of possible wave vectors which are, however, commensurable. Various kinetic processes occurring in the sinusoidal phase have been discussed: squeezing, free expansion, and drift. A dependence of the wave vector on the temperature is enforced by the quite distinct wave vectors describing the ground state and the modulated phase near T_c. We find that a dramatic change of the wave vector occurs in a fairly narrow temperature range (from about 0.8 T_c to 0.9 T_c for $-J_2/J_1 = 0.6$). Third harmonics seem to prevail in the magnetization pattern up to T_c, having been detected unambiguously up to 0.92 T_c. However, the magnitude of the third harmonic component is relatively small, even when the maxima in the magnetization waves are close to saturation.

For values of $-J_2/J_1 > 0.6$ we may anticipate behavior very similar to that reported above but with a correspondingly larger value for the critical wave vector, q_c.[6] Lower values of $-J_2/J_1$, on the other hand, first bring one into the region where the ground state is ferromagnetic (see Fig. 2) and then into the vicinity of the Lifshitz point itself. It may be anticipated that Monte Carlo simulations will show greater fluctuations in these regions: indeed, this is confirmed by some preliminary runs at $-J_2/J_1 = 0.38$ (for which the high-temperature series indicate[6] $k_B T_c/J_1 \simeq 3.53$ and $q_c \simeq 0.77$). Studies on the $6 \times 6 \times 40$ system suggest that the ferromagnetic-to-modulated phase transition takes place somewhat below $k_B T/J_1 = 2.8$. The Fourier transforms of $M(z)$ samples show broad peaks indicative of large equilibrium fluctuations, even for $10 \times 10 \times 40$ systems. However, in contrast to the case $-J_2/J_1 = 0.6$, the wave vector $q(T)$ for $-J_2/J_1 = 0.38$, *drops* from its value at $T = T_c$ when the temperature is reduced. It is planned to study this phenomenon in further detail and also to investigate the two-dimensional version of the model.

ACKNOWLEDGMENTS

One of us (W. S.) is indebted to the Deutsche Forschungsgemeinschaft for the award of a Fellowship; likewise, M. E. F. is indebted to the John Simon Guggenheim Foundation for a Fellowship award. The support of the NSF through the Materials Science Center at Cornell University is gratefully acknowledged. We have enjoyed conversations with Dr. Per Bak about his related work with Dr. J. von Boehm.

APPENDIX: GROUND STATE

Since the exchange interactions in the xy layers are of ferromagnetic sign [see the Hamiltonian (1)], the problem of determining the ground state reduces to that for the Ising model of a linear chain with nearest and next-nearest-neighbor interactions

$$\mathcal{H} = -\tfrac{1}{2} \sum_z (J_1 s_z s_{z\pm 1} + J_2 s_z s_{z\pm 2}) \ , \tag{A1}$$

where s_z corresponds to $s_{x,y,z}$ in Eq. (1). Using the transfer matrix (screw) method, the ground-state energy per spin can be calculated quite easily from Ref. 20, where the case (iii), Sec. II, has been discussed. The four-by-four matrix is[20]

$$\begin{bmatrix} e^{K_1+K_2} & e^{K_1-K_2} & 0 & 0 \\ 0 & 0 & e^{-K_1+K_2} & e^{-K_1-K_2} \\ e^{-K_1-K_2} & e^{-K_1+K_2} & 0 & 0 \\ 0 & 0 & e^{K_1-K_2} & e^{K_1+K_2} \end{bmatrix} , \tag{A2}$$

with $K_1 = J_1/k_B T$ and $K_2 = J_2/k_B T$. The ground-state energy can be found from the solution of the eigenvalue equation

$$\lambda^4 - 2\lambda^3 e^{K_1+K_2} - \lambda^2(e^{-2K_1+2K_2} - e^{2K_1+2K_2}) - \lambda(2e^{-K_1-K_2} - 2e^{-K_1+3K_2}) - (e^{-4K_2} - 2 + e^{4K_2}) = 0 \ . \tag{A3}$$

At zero temperature K_1 and K_2 are infinite. Therefore, in order to determine the eigenvalues λ, one can neglect all terms except λ^4 and the maximum term in the rest of Eq. (A3). The energy per spin, E, follows from the identity ($T = 0$) $E = -k_B T \ln\lambda$. For $J_1, J_2 < 0$ [case (iii)], the lowest energies at zero temperature are

$$E = J_1 - J_2, \quad \text{for } |J_2/J_1| < \tfrac{1}{2} \ , \text{ and} \tag{A4a}$$

$$E = J_2, \quad \text{for } |J_2/J_1| > \tfrac{1}{2} \ , \tag{A4b}$$

where Eq. (A4a) represents the antiferromagnetic state and Eq. (A4b) refers to the (2,2) antiphase state. Likewise, for $J_1 > 0$, $J_2 < 0$ [case (iv)], one gets

$$E = -J_1 - J_2, \quad \text{for } |J_2|/J_1 < \tfrac{1}{2}, \text{ and} \tag{A5a}$$

$$E = J_2, \quad \text{for } |J_2|/J_1 > \tfrac{1}{2}, \tag{A5b}$$

where Eqs. (A5a) and (A5b) represent the ferromagnetic and the (2,2) antiphase state, respectively.

The nature of the various ground states can be checked from the structure of the eigenvectors or, more concretely, by examining the configurations generated by the matrix from the initial states "up-up" and "up-down" in the limit $T \to 0$.

---

*On leave from Fachrichtung Theoretische Physik, Universität des Saarlandes, Saarbrücken, Federal Republic of Germany.

[1]R. J. Elliott, Phys. Rev. 124, 346 (1961).

[2]For similar models see, e.g., J. Yoshimori, J. Phys. Soc. Jpn. 14, 807 (1959); A. Herpin, P. Meriel, and J. Villain, J. Phys. Radium 21, 67 (1960); U. Enz, Physica (Utrecht) 26, 698 (1960).

[3]M. Habenschuss, C. Stassis, S. K. Sinha, H. W. Deckman, and F. H. Spedding, Phys. Rev. B 10, 1021 (1974).

[4]See, e.g., J. W. Cable, E. O. Wollan, W. C. Koehler, and M. K. Wilkinson, Phys. Rev. 140, 1896 (1965); T. O. Brun, S. K. Sinha, N. Wakabayashi, G. H. Lander, L. R. Edwards, and F. H. Spedding, Phys. Rev. B 1, 1251 (1970); D. Gignoux, J. C. Gomez-Sal, R. Lemaire, and A. deCombarieu, Solid State Commun. 21, 637 (1977).

[5]R. M. Hornreich, M. Luban, and S. Shtrikman, Phys. Rev. Lett. 35, 1678 (1975).

[6]S. Redner and H. E. Stanley, Phys. Rev. B 16, 4901 (1977); J. Phys. C 10, 4765 (1977).

[7]W. Selke, Z. Phys. B 29, 133 (1978).

[8]However, attention should be drawn to some interesting work by J. von Boehm and Per Bak, Phys. Rev. Lett. 42, 122 (1979), who have discussed the variation of the wave vector in the modulated phase for a special case of the model [namely, case (iii) $J_1, J_2 < 0$: see Sec. II below]. They employ a more sophisticated layer-by-layer mean-field treatment and compare their results for the temperature dependence of the wave vector with a "devil's-staircase". More recently they have considered case (iv), $J_1 < 0$, $J_2 > 0$, on which we concentrate attention (see Sec. II below); their preliminary results appear to agree with some of our own findings.

[9]K. Binder, in *Monte Carlo Methods in Statistical Physics: Topics in Current Physics,* edited by K. Binder (Springer, Berlin, 1979), Vol. 7, Sec. 1.

[10]K. Binder and P. C. Hohenberg, Phys. Rev. B 6, 3461 (1972); K. Binder and H. Müller-Krumbhaar, Phys. Rev. B 7, 3297 (1973).

[11]M. E. Fisher, in *Critical Phenomena,* Enrico Fermi International School of Physics, Varenna, 1970, edited by M. S. Green (Academic, New York, 1971), Sec. V.

[12]D. P. Landau, Phys. Rev. B 14, 255 (1976).

[13]M. E. Fisher and A. E. Ferdinand, Phys. Rev. Lett. 19, 169 (1967); Phys. Rev. 185, 832 (1969).

[14](a) H. Au-Yang and M. E. Fisher, Phys. Rev. B 11, 3469 (1975); (b) T. W. Capehart and M. E. Fisher, Phys. Rev. B 13, 5021 (1976).

[15]M. Droz and M. D. Coutinho-Filho, in *Proceedings of the 21st Conference on Magnetism and Magnetic Materials, Philadelphia, 1975,* edited by J. J. Becker, G. H. Lander, and J. J. Rhyne, AIP Conf. Proc. No. 29 (AIP, New York, 1976), p. 465.

[16]J. Als-Nielsen, R. J. Birgeneau, M. Kaplan, J. D. Litster, and C. R. Safinya, Phys. Rev. Lett. 39, 1668 (1977).

[17]R. G. Manley, *Waveform Analysis* (Chapman and Hall, London, 1945).

[18]H. Miwa and K. Yosida, Prog. Theor. Phys. 26, 693 (1961).

[19]A. Michelson, Phys. Rev. B 16, 577 (1977).

[20]T. Oguchi, J. Phys. Soc. Jpn. 20, 2236 (1965).